Published in final edited form as:

Eur J Nucl Med Mol Imaging. 2021 November ; 48(12): 3940–3950. doi:10.1007/s00259-021-05386-0.

Prognostic value of [^{18}F]FDG PET/CT in patients with CNS lymphoma receiving ibrutinib-based therapies

Simone Krebs[1], **Audrey Mauguen**[2], **Onur Yildirim**[3], **Vaios Hatzoglou**[3], **Jasmine H. Francis**[4], **Lauren R. Schaff**[5], **Ingo K. Mellinghoff**[5], **Heiko Schöder**[#1,*], **Christian Grommes**[#5,*]

[1]Molecular Imaging and Therapy Service, Department of Radiology, Memorial Sloan Kettering Cancer Center, New York, NY;

[2]Department of Epidemiology and Biostatistics, Memorial Sloan Kettering Cancer Center, New York, NY;

[3]Neuroradiology Service, Department of Radiology, Memorial Sloan Kettering Cancer Center, New York, NY;

[4]Ophthalmic Oncology Service, Department of Surgery, Memorial Sloan Kettering Cancer Center, New York, NY;

[5]Department of Neurology, Memorial Sloan Kettering Cancer Center, New York, NY

[#] These authors contributed equally to this work.

Abstract

Purpose: Current clinical and imaging tools remain suboptimal for predicting treatment response and prognosis in CNS lymphomas. We investigated the prognostic value of baseline [^{18}F]FDG PET in patients with CNS lymphoma receiving ibrutinib-based treatments.

Methods: Fifty-three patients enrolled in a prospective clinical trial and underwent brain PET before receiving single-agent ibrutinib or ibrutinib in combination with methotrexate with or without rituximab. [^{18}F]FDG uptake in these lesions was quantified by drawing PET volumes of interest around up to five [^{18}F]FDG-avid lesions per patient (with uptake greater than surrounding brain). We measured standardized uptake values (SUV_{max}), metabolic tumor volumes, total lesion glycolysis (TLG), and the sum thereof in these lesions. We analyzed the relationship between PET parameters and mutation status, overall response rates, and progression-free survival (PFS).

[*]**Corresponding author**: Heiko Schöder, Molecular Imaging and Therapy Service, Memorial Sloan Kettering Cancer Center, 1275 York Ave, Box 77, New York, NY 10065; schoderh@mskcc.org.

Authors' contributions: Conceived and designed the study: S.K., C.G., and H.S.; collected, analyzed, and interpreted the data: S.K., A.M., O.Y., V.H., J.H.F., L.R.S., I.K.M., C.G., and H.S.; performed statistical analysis: A.M.; wrote the manuscript: S.K., C.G., and H.S.; reviewed the data and edited and approved the final version of the manuscript: all authors.

Conflicts of interest/Competing interests: C.G. reports consulting for BTG International and Kite. The remaining authors have no competing interests.

Ethical approval: All procedures involving human participants were performed in accordance with the ethical standards of the institutional and/or national research committee and with the 1964 Helsinki declaration and its later amendments or comparable ethical standards.

Informed consent: Informed written consent was obtained from all individual participants included in the study.

(NCT02315326; https://clinicaltrials.gov/ct2/show/NCT02315326?term=NCT02315326&draw=2&rank=1)

Results: Thirty-eight patients underwent single-agent therapy and 15 received combination therapy. On PET, 15/53 patients had no measurable disease. In the other 38 patients, a total of 71 lesions were identified on PET. High-intensity [^{18}F]FDG uptake and a larger volume of [^{18}F]FDG-avid disease were inversely related to treatment outcome ($p \leq 0.005$). In univariable analysis, PFS was linearly correlated with all PET parameters, with stronger association when sum-values were used. A multivariable model showed that risk of progression increased by 9% for every 5-unit increase in sumSUV$_{max}$ (hazard ratio = 1.09 [95% CI: 1.04 to 1.14]).

Conclusion: Higher lesional metabolic parameters are inversely related to outcome in patients undergoing ibrutinib-based therapies, and sumSUV$_{max}$ emerged as a strong independent prognostic factor.

Keywords

[^{18}F]FDG; PET; ibrutinib; CNS lymphoma; imaging pattern

INTRODUCTION

Primary CNS lymphoma is a rare but aggressive form of extra-nodal non-Hodgkin lymphoma limited to the brain, spinal cord, leptomeninges, or eyes. With an incidence of 0.44 per 100,000, CNS lymphoma accounts for approximately 2% of all primary CNS tumors in the US [1, 2]. Histologically, CNS lymphoma presents in most cases (90%) as diffuse large B-cell lymphoma (DLBCL), occasionally as Burkitt lymphoma, low-grade lymphoma, or T cell lymphoma [3]. In contrast, “secondary” CNS lymphoma is defined as CNS involvement that can be seen in a subset of patients with primarily systemic DLBCL.

[^{18}F]-fluorodeoxyglucose ([^{18}F]FDG; FDG) PET is a critical tool for staging and response assessment in many subtypes of systemic lymphoma [4, 5], but its utility in CNS lymphoma is not as well established. Whereas cortical brain shows high FDG uptake (potentially interfering with the detection of FDG-avid brain lesions), most sites of CNS lymphoma are in fact located in the white matter, near deep cerebral structures or in periventricular regions, suggesting that [^{18}F]FDG PET may also be useful in diagnosis and follow-up of this disease [6, 7]. This may be particularly relevant in patients who do not respond to standard therapy, consisting of high-dose methotrexate (HD-MTX)-based chemotherapy [8]. Indeed, disease recurrence is common, and other patients may have refractory disease that fails to respond to this first-line therapy. In these patients with relapsed or refractory (r/r) CNS lymphoma, ibrutinib, a small molecule Bruton-Tyrosine kinase (BTK) inhibitor, has emerged as a promising agent [9–12].

Current clinical and imaging tools are of limited value for the prediction of treatment response and patient outcome in CNS lymphomas. In this study, we set out to explore the potential prognostic utility of baseline [^{18}F]FDG PET/CT in patients with primary and secondary CNS lymphoma receiving ibrutinib-based treatments.

MATERIALS AND METHODS

Clinical study

As part of a prospective research protocol approved by the Institutional Review Board, patients with r/r CNS lymphoma were imaged with [^{18}F]FDG PET/CT prior to ibrutinib-based treatment. All procedures were performed in accordance with the ethical standards of the institutional and/or national research committee and with the 1964 Helsinki declaration and its later amendments or comparable ethical standards. All patients provided written informed consent [NCT02315326]. Eligible patients had r/r primary or secondary CNS lymphoma or newly diagnosed secondary CNS lymphoma and were ≥18 years old with an Eastern Cooperative Oncology Group (ECOG) performance status ≤2, normal end-organ function, and an unrestricted number and type of prior therapies. In patients with secondary CNS lymphoma, systemic disease needed to be absent. Baseline disease assessments to evaluate disease burden followed the International Primary CNS Lymphoma Collaborative Group (IPCG) guidelines [13] and included brain MRI, total spine MRI, cerebrospinal fluid (CSF) collection, ophthalmologic examination, and whole-body PET with [^{18}F]FDG. Participants with r/r primary or secondary CNS lymphoma were assigned to cohorts of increasing oral daily doses of ibrutinib (560 mg, 840 mg) or a combination regimen of ibrutinib with high-dose methotrexate (HD-MTX) with or without rituximab (HD-MTX was given at 3.5 g/m2 every two weeks for a total of eight doses) [9, 10]. Patients with newly diagnosed secondary CNS lymphoma underwent combination treatment.

[^{18}F]FDG PET/CT imaging protocol

Before injection of [^{18}F]FDG, all patients fasted for at least six hours. The median administered activity was 449.55 MBq (12.15 mCi); IQR: 58.46 MBq (1.58 mCi), following a median uptake time of 85 min (IQR: 34 min). Median blood sugar level was 95 mg/dl (IQR: 23 mg/dl). Patients were scanned while in the supine position. In 51/53 patients, a dedicated brain PET/CT scan was obtained in addition to a body PET/CT from skull base to thighs. Two patients were scanned from skull vertex to feet without performing a dedicated brain PET/CT—one patient at our center and one patient at an outside institution. Fifty patients were imaged using systems of the GE Discovery series (VCT, 690, 710), one patient with a Siemens Biograph 128, and two patients with unspecified time-of-flight PET/CT scanners at outside institutions. Cross-calibration between the dose calibrator and PET scanners was performed monthly at our institution. Low-dose CT images obtained during PET/CT were used for attenuation correction of the PET emission scan and for anatomical orientation. PET/CT images were reconstructed using an ordered-subsets expectation maximization algorithm and a Gaussian filter using the standard manufacturer-supplied reconstruction software. The acquisition and reconstruction parameters were harmonized to minimize differences in standardized uptake values (SUVs) between scanners and keep them within 10%, as tested using measurements of the IEC image quality phantom. For brain PET/CT, a spiral CT was acquired using a full helical acquisition at 1 sec/rotation, 150 mA, 120–140 kV with slice thickness of 3.75 mm. Immediately upon completion of the CT, a 10-min 3D PET scan was acquired. CT and PET data were reconstructed using a 30-cm transaxial field of view.

PET image interpretation and data analysis

A board-certified nuclear medicine physician defined regions of interest (ROIs) for the lesions and normal brain on a GE Advantage workstation using PET VCAR software. The [^{18}F]FDG PET/CT was windowed to visualize the focal FDG avidity associated with the known brain lesion on MRI then an ROI was placed to encompass the entire area of abnormal FDG avidity. One patient had leptomeningeal disease involvement in the spinal canal that was seen on body PET. Lesions were defined as *PET-positive* if both imaging specialist investigators, nuclear medicine physician and radiologist, were able to unambiguously identify the lesions on the PET images in a joint visual assessment. Lesion volumes were measured by performing three-dimensional threshold-based volume of interest (VOI) analyses for the FDG uptake in all patients. Tracer uptake was quantified by SUVs normalized to patients' body weight. For lesion VOI, SUV_{max} was recorded in addition to SUV_{mean}. SUV_{max} referred to the voxel with the maximum intensity of FDG uptake in the VOI. We determined the maximum standardized uptake values (SUV_{max}), metabolic tumor volumes (MTV; volume encompassed by a 42% isocontour around the voxel with the highest PET uptake) [14], and total lesion glycolysis (TLG; calculated by multiplying MTV by SUV_{mean}). Additional VOIs were then drawn in comparable contralateral normal brain, including cortical brain and subcortical brain, and in contralateral white matter. For normal brain, only SUV_{mean} within the VOI was used. We determined the sum of SUV_{max} ($sumSUV_{max}$), MTV (sumMTV), and TLG (sumTLG) in up to five target lesions as a simplified measure of patient tumor burden and metabolic activity (Supplementary Figure S1). In patients with more than 5 lesions (n=3), the largest lesions were considered. For patients whose lesions did not show FDG uptake higher than background local white matter (*PET-negative*), we used the average SUV_{mean} of normal white matter in this cohort in the quantitative analyses.

MR imaging protocol and lesion measurement

All sequences were acquired on 1.5T or 3T scanners (Signa Excite, HDx and Discovery 750, GE Healthcare, Milwaukee, WI) using an 8-channel head coil. Gadopentetate dimeglumine (Magnevist; Bayer HealthCare Pharmaceuticals, Wayne, NJ) was injected via an intravenous catheter (18–21 gauge) at doses standardized by patient body weight (0.2 mL/kg body weight, maximum 20 mL) at 2–3 mL/s. Further details regarding imaging acquisition and processing have been previously reported [15]. For lesion measurements on MRI, corresponding lesions were identified by a board-certified radiologist on axial and sagittal T1-weighted post-contrast images and three-dimensional measurements were performed. In cases of PET-positive lesions without correlate on post-contrast T1-weighted images, fluid attenuation inversion recovery (FLAIR) images were inspected. The median interval between MRI and PET was 5 days (IQR: 7 days).

Treatment response assessments

Evaluation of treatment response followed the IPCG guidelines [13]. Response to treatment was assessed in all CNS compartments using MRI imaging and CSF cytology, as well as ophthalmologic examination in case of eye involvement. Assessment of radiographic

response was done independently by a board-certified neuroradiologist and a board-certified ophthalmologist. Overall response rate (ORR) was based on IPCG criteria.

Statistical analysis

Patient data was summarized using descriptive statistics, including median (range) for continuous variables and frequency and percentage for categorical variables, unless otherwise specified. Boxplots were used to graphically describe the distribution of the PET parameters. PET parameters and tumor size were correlated using Spearman (non-linear) and Pearson (linear) correlation coefficients. To ensure the validity of the estimate of the Pearson coefficient, a logarithm transformation of the variables (tumor size and PET parameters) was performed. The confidence intervals (95% CI) for correlations were calculated according to the method of Bonett and Wright [16]. Distribution of the PET parameters was compared by mutation status for MYD88 and CD79B using a Mann-Whitney-Wilcoxon test. The presence of an increasing trend of PET parameter values with response (CR, PR, and SD/PD) was assessed using Kruskal-Wallis tests. A p-value of 0.05 or less was considered significant. PFS was calculated from trial registration until disease progression or death. Surviving patients without disease progression were censored at the date of their last clinical assessment. PFS curve and median PFS were estimated using a Kaplan-Meier estimator. Association between clinical factors and PET parameters with PFS were assessed through univariable and multivariable Cox proportional hazard models. Variables with $p <= 0.10$ in univariable were entered in the multivariable model. A backward variable selection was performed to keep variables associated to PFS with $p <= 0.05$. Hazard ratios (HR) are presented with 95% confidence intervals (95% CI). In outcome analyses (response and PFS), for PET-negative patients we used as inputs for SUV the average SUV_{mean} of normal white matter in this cohort (i.e. reference background activity, $SUV_{mean} = 3$). For MTV and TLG a 0 value was set, and the data were included in the analyses. Additional analyses were performed for the subset of patients with PET-positive lesions and included in the supplementary data.

RESULTS

Fifty-three patients underwent baseline [^{18}F]FDG PET/CT within three weeks of initiation of the ibrutinib-based treatment (Figure 1). Patient characteristics are summarized in Table 1. Thirty-four patients had been diagnosed with primary CNS lymphoma and 19 patients with secondary CNS lymphoma; 50 of the 53 patients had relapsed or refractory (r/r) disease, and three patients had newly diagnosed secondary CNS lymphoma. Thirty-eight patients were treated with increasing oral daily doses of ibrutinib (3 at 560 mg daily; 35 at 840 mg daily), while 15 patients received HD-MTX in combination with ibrutinib (9 also received rituximab). Of the 53 patients, 22 received corticosteroids at the time of imaging.

Imaging patterns and [^{18}F]FDG PET parameters

PET-positive lesions were found in 38/53 patients (Figure 2, A and B). A total of 71 lesions were examined (n=5, 5 pts; n=4, 1 pt; n=3, 2 pts; n=2, 6 pts; n=1, 24 pts) (median 1, range: 0–5). Lesion sites included cortico-subcortical/white matter (n=42), ependymal/subependymal (n=4), intraventricular (n=7), basal ganglia (n=3), cerebellum (n=7), and

leptomeningeal (n=8). No lesion was strictly located in the cortex. Lesion heterogeneity on PET and T1-weighted images in a few lesions were noted (Supplementary Figure S2A).

Of the 15 PET-negative patients, 2 patients had no abnormality on post-contrast T1-weighted MRI and had leptomeningeal disease diagnosed in cerebrospinal fluid (CSF) analysis. In 3 other patients, MR showed non-masslike, non-measurable ill-defined patchy enhancements within the centrum semiovale (left greater than right) and body of the corpus callosum, or only patchy ependymal/subependymal enhancement along the right occipital horn. In the remaining 10 patients, MRI revealed sites of abnormal T1-Gd enhancement (Figure 2C, Supplementary Figure S2B). In retrospect, in one of these 10 patients, an FDG-avid lesion might have been obscured by the physiologic intense uptake in basal ganglia (Supplementary Figure S2C). In the other 9 patients, the lack of appreciable FDG uptake was possibly related to small lesion volume (on MRI: median 0.6 cm^3, range: 0.1–1.7 cm^3).

On the contrary, three FDG-avid lesions (SUV_{max} of 18, 12, and 11, respectively) seen in two patients had no correlate on post-contrast T1-weighted and FLAIR images (Supplementary Figure S2D), and five FDG-avid lesions in three patients were non-measurable on MRI (e.g., due to leptomeningeal disease in the spinal canal or linear and nodular non-masslike enhancement). Furthermore, involvement of the choroid plexus was partly better seen on PET than on MRI due to physiologic contrast enhancement in this region (Supplementary Figure S2E). Leptomeningeal involvement of cranial nerves was partly seen on PET (Supplementary Figure S2F).

Lesion uptake was variable with a median SUV_{max} of 19 (range: 3–48) across all 53 patients. The median values for the sum of SUV_{max} ($sumSUV_{max}$), MTV (sumMTV), and TLG (sumTLG) were 20 (range: 3–157), 2 cm^3 (range: 0–37), and 21 (range: 0–787), respectively, in the 53 patients.

Overall, PET-positive patients had significantly larger lesions than PET-negative patients (mean volume 4.0 ± 6.6 cm^3, range 0.01–42.0 and 0.6 ± 0.6 cm^3, range 0.1–1.7; p=0.03; two-tailed Mann-Whitney test). Although partial volume averaging effects inevitably lead to an underestimation of FDG uptake in small lesions, only moderate correlation between lesion volume and PET parameters was noted (Supplementary Table S1).

PET parameters were not associated with cellularity or amount of protein in CSF collected at the time of study inclusion.

Association of [^{18}F]FDG PET/CT parameters and molecular determinants for clinical response to ibrutinib

Overall, 28 of 50 (56%) patients had known mutations in MYD88, and 21 of 51 (41%) had a mutation in CD79B. There was no significant difference in the distribution of PET parameters according to MYD88 or CD79B mutation status (Supplementary Tables S2 and S3).

Association of [^{18}F]FDG PET/CT parameters with treatment response and patient outcome

Response to treatment was assessed in all CNS compartments using MRI and CSF cytology, as well as ophthalmologic examination in case of eye involvement. ORR was based on IPCG criteria. A total of 40 of 53 (75%) patients had a clinical response, including 24 patients with a complete response (CR) and 16 patients with a partial response (PR). Six patients had stable disease (SD) and seven patients experienced progressive disease (PD). For subsequent analyses, SD and PR were grouped as non-responders due to their small frequencies. Figure 3 depicts the distribution of PET parameters in these subgroups, showing increasing PET values in patients with PR and non-responders as compared to CR. Both SUV_{max} and $sumSUV_{max}$ were negatively associated with response ($p=0.002$ and $p<0.001$, respectively), as were MTV and sumMTV ($p=0.02$ and $p=0.005$, respectively) and TLG and sumTLG ($p=0.01$ and $p=0.004$, respectively) (Supplementary Table S4).

The median follow-up time in all 53 patients was 39.6 months (range, 16.3–57.5). The median PFS was 8.7 months (range, 0.9–33.7) (Supplementary Figure S3).

In univariable analysis for all 53 patients, all PET parameters showed an inverse linear association with the risk of progression/death, with a stronger association upon using the sum-values, which were therefore used in the subsequent multivariable analysis (Table 2).

Besides PET parameters, single-agent treatment was associated with a higher risk of progression/death as compared to combination treatment in the 53 patients ($p=0.01$, HR=3.09, 95% CI 1.18–8.09); patients with larger tumor volumes on MRI also had a higher risk ($p=0.05$, HR=1.16, 95% CI 0.99–1.35) (Table 2).

Patients with positive baseline PET/CT had a higher tendency for the risk of progression/death than patients with negative PET/CT, although not statistically significant ($p=0.19$).

Known clinical risk factors – at least in the upfront setting, such as age and ECOG [17], as well as MYD88 and CD79B mutations, known molecular determinants associated with clinical response to ibrutinib, were not significantly associated with the risk of progression/death in our study.

In multivariable analysis for all 53 patients, the risk of progression increased by 9% for every 5-unit increase in $sumSUV_{max}$ ($p < 0.001$, HR=1.09, 95% CI 1.04–1.14). The risk of progression/death more than doubled for patients receiving a single agent as compared to combination therapy ($p=0.02$, HR=2.73, 95% CI 1.03–7.25).

The results of the additional analyses performed for the subset of 38 PET-positive patients are shown in Supplementary Figures S4 and S5 and Supplementary Tables 5–12. Treatment (single agent versus combination therapy) was not associated with PFS, possibly due to smaller sample size. Overall, similar results were found in both analyses, for the entire cohort of 53 patients and the subgroup of 38 patients with clearly PET-positive lesions, supporting the robustness of our results.

DISCUSSION

This study shows that baseline [^{18}F]FDG PET/CT provides prognostic information in patients with CNS lymphoma and predicts response to ibrutinib-based treatments: High-intensity [^{18}F]FDG uptake and a larger volume of [^{18}F]FDG-avid disease were inversely related to response to ibrutinib in CNS lymphoma, and were quantitatively related to the risk of disease progression or death. In particular, sumSUV$_{max}$ emerged as an independent prognostic factor in this setting. These findings are clinically relevant since early prediction of outcome remains particularly challenging in patients with CNS lymphoma. To date, no imaging or laboratory testing has been identified to address this question. While age and performance status are well established prognostic parameters for newly diagnosed patients, no such markers exist for patients with recurrent/refractory disease.

Molecular imaging of CNS lymphoma may potentially improve early diagnosis and monitoring of response or, as shown in our study, provide clinically relevant prognostic information. For instance, patients with expected poor prognosis and/or those who are unlikely to respond to current regimens may benefit from early enrollment in clinical trials with emerging therapies, such as CD19-targeted CAR T cell therapies [18, 19] or closer follow-up for earlier detection of relapse.

[^{18}F]FDG PET is currently the main molecular imaging test for the evaluation of primary CNS lymphoma, but it offers only moderate sensitivity and specificity for diagnosing all primary CNS lymphoma sites [20]. While we observed FDG-avid lesions in 38/53 (72%) of our patients, concordant with other reports [6, 7], PET imaging was negative in the other 15 patients. In 2 of these 15 patients, the MRI was also negative (i.e., diagnosis based on CSF cytology), and in the other 13 patients, the PET-negative lesions seen only on MR showed patchy contrast enhancement or were small, linear, or nodular, mostly in ependymal/subependymal sites, or were patchy and ill-defined. The influence of lesion size on detection on PET has been reported [21]. On the other hand, we encountered a few PET-positive lesions whose structural correlates on MR may have been easily overlooked; for instance, due to their proximity to the choroid plexus, which shows physiologic intense contrast enhancement, or without clear abnormality on T1w-post-contrast and FLAIR images. Altogether, these observations suggest that combined PET/MRI is the ideal modality for comprehensive imaging characterization of CNS lymphoma. Of note, adding the PET component to the MRI does not result in additional scanning time. Also, for purely diagnostic purposes, radiolabeled amino acids or other small molecule-based tracers may potentially aid in detecting smaller CNS lymphoma lesions [22]. However, currently, none of these agents are approved for use in brain tumors or CNS lymphoma in the US [23].

In our study, all PET parameters, especially sum-values, were strongly associated with risk of progression, with sumSUV$_{max}$ as the strongest independent prognostic factor. While SUVs and tumor burden measured on [^{18}F]FDG PET/CT have been identified as prognostic factors in patients with systemic lymphoma [24–27], data in CNS lymphoma are still relatively sparse. A few studies, mostly retrospective, have explored the prognostic role of [^{18}F]FDG PET in this setting [7, 28–30]. For instance, one retrospective study in 52 patients with untreated primary CNS lymphoma reported shorter PFS and OS in patients

with larger MTV (cut-off 9.8 cm^3) and higher total lesion glycolysis (TLG) [7]. Another retrospective study in 42 patients with newly diagnosed primary CNS lymphoma found an inverse correlation between high uptake on pretreatment [^{18}F]FDG PET and survival [29]. A more recent retrospective study in a small sample of 14 patients with primary CNS lymphoma reported that only TLG provided prognostic information [30]. In this context, our study is one of the largest and benefited from prospective patient enrollment in a clinical trial with prespecified imaging time points, the fact that all patients underwent [^{18}F]FDG-PET, and the application of a new drug regimen. Going forward, our data may provide clinical guidance for patients with r/r CNS lymphoma, as baseline [^{18}F]FDG PET could serve as an early tool to identify those patients (with high sumSUV_{max}) who are likely to show only limited, or possibly even no, clinical response to ibrutinib-based therapy, suggesting that they should be considered for other clinical trials.

Although new therapeutic regimens have improved the survival of patients with CNS lymphoma, management of this disease remains challenging, particularly in elderly patients and those with r/r disease. Ibrutinib, a small molecule targeting BTK that mediates downstream signals of MYD88 and CD79B, has emerged as a promising treatment approach for CNS lymphoma. Activating mutations in MYD88 and CD79B are frequently found in primary CNS lymphoma. We found no difference in the distribution of PET parameters based on MYD88 or CD79B mutation status and no correlation with ORR, possibly due to the still relatively limited sample size. Nevertheless, these findings are in alignment with the lack of complete response to ibrutinib in patients with primary CNS lymphoma with concurrent mutations in MYD88 and CD79B and the observation of complete response in patients without mutations. In contrast, the correlation of mutations in these driver genes with response in lymphoma outside the brain with response has been confirmed in multiple studies. In this regard, the availability of reliable imaging surrogates predictive of response to ibrutinib-based treatments could facilitate patient selection. The response rate to ibrutinib observed in patients with CNS lymphoma is substantially higher [9] than in those with systemic DLBCL (25% ORR to single-agent ibrutinib; PFS: 2 months) [31]. In view of the prognostic value of [^{18}F]FDG PET in patients with primary and secondary CNS lymphoma receiving ibrutinib-based treatment, further evaluation of its utility in patients with systemic lymphoma may be suggested – especially in the absence of known mutational status in the driver genes MYD88 and CD79B.

CNS lymphoma lesions mostly show high [^{18}F]FDG uptake, due to increased glucose metabolism as compared to normal brain tissue. This demand is met by enhanced cellular entry of nutrients through upregulation of specific transporters and enzymes. Tumor cells frequently overexpress glucose transporter GLUT1 and GLUT3 as well as hexokinase II [32, 33]. The utility of using [^{18}F]FDG PET in patients with CNS lymphoma is supported by the recent discovery of the hyperactive RelA/p65-hexokinase 2 signaling axis, promoting lymphomagenesis and tumor progression [34]. Distinct molecular alterations related to mutated MYD88/CD79B in immunocompetent CNS lymphoma converge to deregulate RelA/p65 expression and drive glycolysis, which is critical for intracerebral tumor progression and [^{18}F]FDG-PET imaging. Thus, [^{18}F]FDG PET enables interrogation of the functional contribution of these genomic alterations to tumor progression, which are not readily identified by genotypic or transcriptomic analyses.

Our study had some limitations. First, patients had received a variety of prior treatment regimens, which may have affected outcome. Second, two treatment subgroups, single agent with ibrutinib vs. ibrutinib combination therapy, were included in this analysis, one of which was substantially larger, and we only studied patients receiving ibrutinib. Third, while most patients had r/r disease, some received ibrutinib combination therapy upfront in the first-line setting. Nevertheless, in view of the relatively low incidence of CNS lymphoma, our study was comparatively large, and all patients were enrolled prospectively. Furthermore, in both analyses - for the entire cohort of 53 patients as well as for the subgroup of the 38 patients with clearly PET-positive lesions – sumSUVmax emerged as the strongest independent prognostic factor, supporting the robustness of our results. Finally, PET and MRI were acquired separately; however, they were reviewed simultaneously by two imaging experts in consensus. We realize that quantitative parameters derived from dynamic contrast-enhanced MRI and diffusion-weighted imaging may also provide prognostic information in patients with primary CNS lymphoma [15]. Therefore, and because of the complementary information derived from MR and molecular imaging probes, combined PET/MR is likely the ideal method for characterization of this disease and, where available, should be employed going forward, at least during initial staging.

CONCLUSION

Baseline [^{18}F]FDG PET provides prognostic information in patients with r/r CNS lymphoma receiving ibrutinib-based treatments: Higher metabolic values predict a worse outcome, with sumSUVmax as a strong independent prognostic factor for PFS. [^{18}F]FDG-PET should be incorporated into future prospective trials in CNS lymphoma to confirm its prognostic value and study its role in response assessment.

Supplementary Material

Refer to Web version on PubMed Central for supplementary material.

Acknowledgment:

We thank Leah Bassity for her expert editorial support.

Funding:

This work was supported by a research grant from Pharmacyclics to MSK. Pharmacyclics was not involved in the design or conduct of the study. The statistical analysis plan and data analyses were performed by MSK investigators. This study was partially supported by the National Institutes of Health/National Cancer Institute Cancer Center Support Grant [P30 CA008748], National Institutes of Health/National Cancer Institute Paul Calabresi Career Development Award for Clinical Oncology [K12 CA184746 to S.K.], and National Institutes of Health MSK SPORE in Lymphoma [P50 CA192937 to S.K.], as well as by grants from Cycle for Survival Equinox (C.G.) and the Leukemia & Lymphoma Society (C.G.).

REFERENCES

1. Ostrom QT, Gittleman H, Xu J, et al.CBTRUS Statistical Report: Primary brain and other central nervous system tumors diagnosed in the United States in 2009–2013. Neuro-Oncol. 2016;18(suppl_5):v1–v75. [PubMed: 28475809]

2. Mendez JS, Ostrom QT, Gittleman H, et al.The elderly left behind-changes in survival trends of primary central nervous system lymphoma over the past 4 decades. Neuro-Oncol. 2018;20(5):687–694. [PubMed: 29036697]
3. Camilleri-Broët S, Martin A, Moreau A, et al.Primary central nervous system lymphomas in 72 immunocompetent patients: pathologic findings and clinical correlations. Groupe Ouest Est d'étude des Leucénies et Autres Maladies du Sang (GOELAMS). Am J Clin Pathol. 1998;110(5):607–612. [PubMed: 9802345]
4. Younes A, Hilden P, Coiffier B, et al.International Working Group consensus response evaluation criteria in lymphoma (RECIL 2017). Ann Oncol. 2017;28(7):1436–1447. [PubMed: 28379322]
5. Cheson BD, Fisher RI, Barrington SF, et al.Recommendations for initial evaluation, staging, and response assessment of Hodgkin and non-Hodgkin lymphoma: the Lugano classification. J Clin Oncol. 2014;32(27):3059–3068. [PubMed: 25113753]
6. Albano D, Bosio G, Bertoli M, Giubbini R, Bertagna F. 18F-FDG PET/CT in primary brain lymphoma. J Neuro-Oncol. 2018;136(3):577–583.
7. Albano D, Bertoli M, Battistotti M, et al.Prognostic role of pretreatment 18F-FDG PET/CT in primary brain lymphoma. Ann Nucl Med. 2018;32(8):532–541. [PubMed: 29982990]
8. Grommes C, DeAngelis LM. Primary CNS lymphoma. J Clin Oncol. 2017;35(21):2410–2418. [PubMed: 28640701]
9. Grommes C, Pastore A, Palaskas N, et al.Ibrutinib unmasks critical role of bruton tyrosine kinase in primary CNS lymphoma. Cancer Discov. 2017;7(9):1018–1029. [PubMed: 28619981]
10. Grommes C, Tang SS, Wolfe J, et al.Phase 1b trial of an ibrutinib-based combination therapy in recurrent/refractory CNS lymphoma. Blood. 2019;133(5):436–445. [PubMed: 30567753]
11. Lionakis MS, Dunleavy K, Roschewski M, et al.Inhibition of B cell receptor signaling by ibrutinib in primary CNS lymphoma. Cancer Cell. 2017;31(6):833–843.e835. [PubMed: 28552327]
12. Soussain C, Choquet S, Blonski M, et al.Ibrutinib monotherapy for relapse or refractory primary CNS lymphoma and primary vitreoretinal lymphoma: Final analysis of the phase II 'proof-of-concept' iLOC study by the Lymphoma study association (LYSA) and the French oculo-cerebral lymphoma (LOC) network. Eur J Cancer (Oxford, England: 1990). 2019;117:121–130.
13. Abrey LE, Batchelor TT, Ferreri AJ, et al.Report of an international workshop to standardize baseline evaluation and response criteria for primary CNS lymphoma. J Clin Oncol. 2005;23(22):5034–5043. [PubMed: 15955902]
14. Erdi YE, Mawlawi O, Larson SM, et al.Segmentation of lung lesion volume by adaptive positron emission tomography image thresholding. Cancer. 1997;80(12 Suppl):2505–2509. [PubMed: 9406703]
15. Hatzoglou V, Oh JH, Buck O, et al.Pretreatment dynamic contrast-enhanced MRI biomarkers correlate with progression-free survival in primary central nervous system lymphoma. J Neuro-Oncol. 2018;140(2):351–358.
16. Bonett DG, Wright TA. Sample size requirements for estimating pearson, kendall and spearman correlations. Psychometrika. 2000;65(1):23–28.
17. Abrey LE, Ben-Porat L, Panageas KS, et al.Primary central nervous system lymphoma: the Memorial Sloan-Kettering Cancer Center prognostic model. J Clin Oncol. 2006;24(36):5711–5. [PubMed: 17116938]
18. Abramson JS, McGree B, Noyes S, et al.Anti-CD19 CAR T cells in CNS diffuse large-B-cell lymphoma. New Engl J Med. 2017;377(8):783–784. [PubMed: 28834486]
19. Frigault MJ, Dietrich J, Martinez-Lage M, et al.Tisagenlecleucel CAR T-cell therapy in secondary CNS lymphoma. Blood. 2019;134(11):860–866. [PubMed: 31320380]
20. Zou Y, Tong J, Leng H, Jiang J, Pan M, Chen Z. Diagnostic value of using 18F-FDG PET and PET/CT in immunocompetent patients with primary central nervous system lymphoma: A systematic review and meta-analysis. Oncotarget. 2017;8(25):41518–41528. [PubMed: 28514747]
21. Mercadal S, Cortés-Romera M, Vélez P, Climent F, Gámez C, González-Barca E. [Positron emission tomography combined with computed tomography in the initial evaluation and response assessment in primary central nervous system lymphoma]. Med Clinica. 2015;144(11):503–506.
22. Herhaus P, Lipkova J, Lammer F, et al.CXCR4-targeted positron emission tomography imaging of central nervous system B-cell lymphoma. J Nucl Med. 2020. Epub ahead of print.

23. Clarke BN. PET radiopharmaceuticals: What's new, what's reimbursed, and what's next?J Nucl Med Technol. 201822;jnmt.117.205021.
24. Vercellino L, Cottereau AS, Casasnovas O, et al.High total metabolic tumor volume at baseline predicts survival independent of response to therapy. Blood. 2020;135(16):1396–1405. [PubMed: 31978225]
25. Ceriani L, Gritti G, Cascione L, et al.SAKK38/07 study: integration of baseline metabolic heterogeneity and metabolic tumor volume in DLBCL prognostic model. Blood Advances. 2020;4(6):1082–1092. [PubMed: 32196557]
26. Bailly C, Carlier T, Berriolo-Riedinger A, et al.Prognostic value of FDG-PET in patients with mantle cell lymphoma: results from the LyMa-PET Project. Haematologica. 2020;105(1):e33–e36. [PubMed: 31371411]
27. Moskowitz AJ, Schöder H, Gavane S, et al.Prognostic significance of baseline metabolic tumor volume in relapsed and refractory Hodgkin lymphoma. Blood. 2017;130(20):2196–2203. [PubMed: 28874350]
28. Kawai N, Zhen HN, Miyake K, Yamamaoto Y, Nishiyama Y, Tamiya T. Prognostic value of pretreatment 18F-FDG PET in patients with primary central nervous system lymphoma: SUV-based assessment. J Neuro-Oncol. 2010;100(2):225–232.
29. Kasenda B, Haug V, Schorb E, et al.18F-FDG PET is an independent outcome predictor in primary central nervous system lymphoma. J Nucl Med. 2013;54(2):184–191. [PubMed: 23249539]
30. Okuyucu K, Alagoz E, Ince S, Ozaydin S, Arslan N. Can metabolic tumor parameters on primary staging (18)F-FDG PET/CT aid in risk stratification of primary central nervous system lymphomas for patient management as a prognostic model?Rev Esp Med Nucl Imagen Mol. 2018;37(1):9–14. [PubMed: 28733137]
31. Wilson WH, Young RM, Schmitz R, et al.Targeting B cell receptor signaling with ibrutinib in diffuse large B cell lymphoma. Nature Med. 2015;21(8):922–926. [PubMed: 26193343]
32. Yamamoto T, Seino Y, Fukumoto H, et al.Over-expression of facilitative glucose transporter genes in human cancer. Biochem Biophys Res Commun. 1990;170(1):223–230. [PubMed: 2372287]
33. Mathupala SP, Ko YH, Pedersen PL. Hexokinase II: cancer's double-edged sword acting as both facilitator and gatekeeper of malignancy when bound to mitochondria. Oncogene. 2006;25(34):4777–4786. [PubMed: 16892090]
34. Tateishi K, Miyake Y, Kawazu M, et al.A hyperactive RelA/p65-hexokinase 2 signaling axis drives primary central nervous system lymphoma. Cancer Res. 2020;80(23):5330–5343. [PubMed: 33067267]

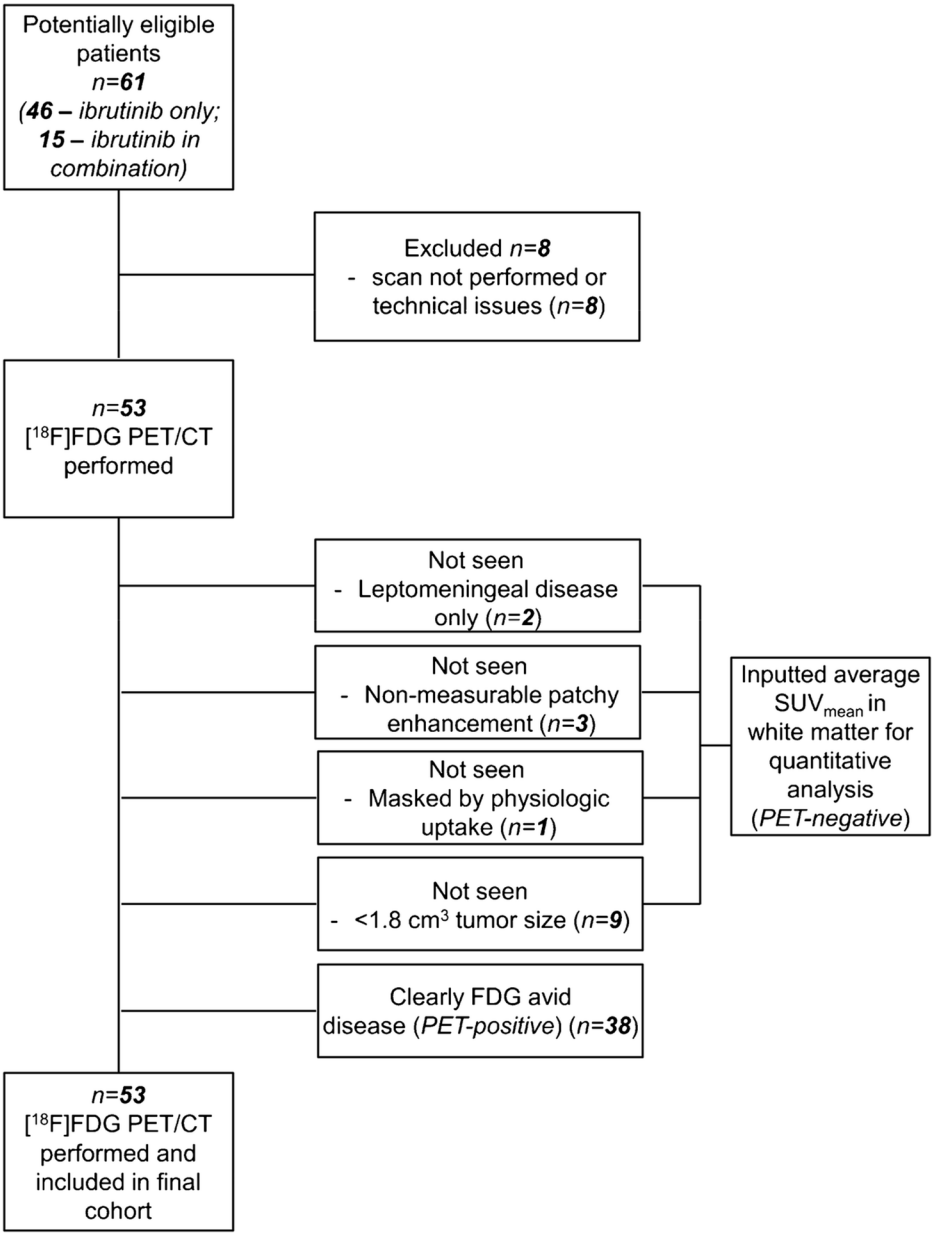

Fig. 1.
CONSORT diagram.

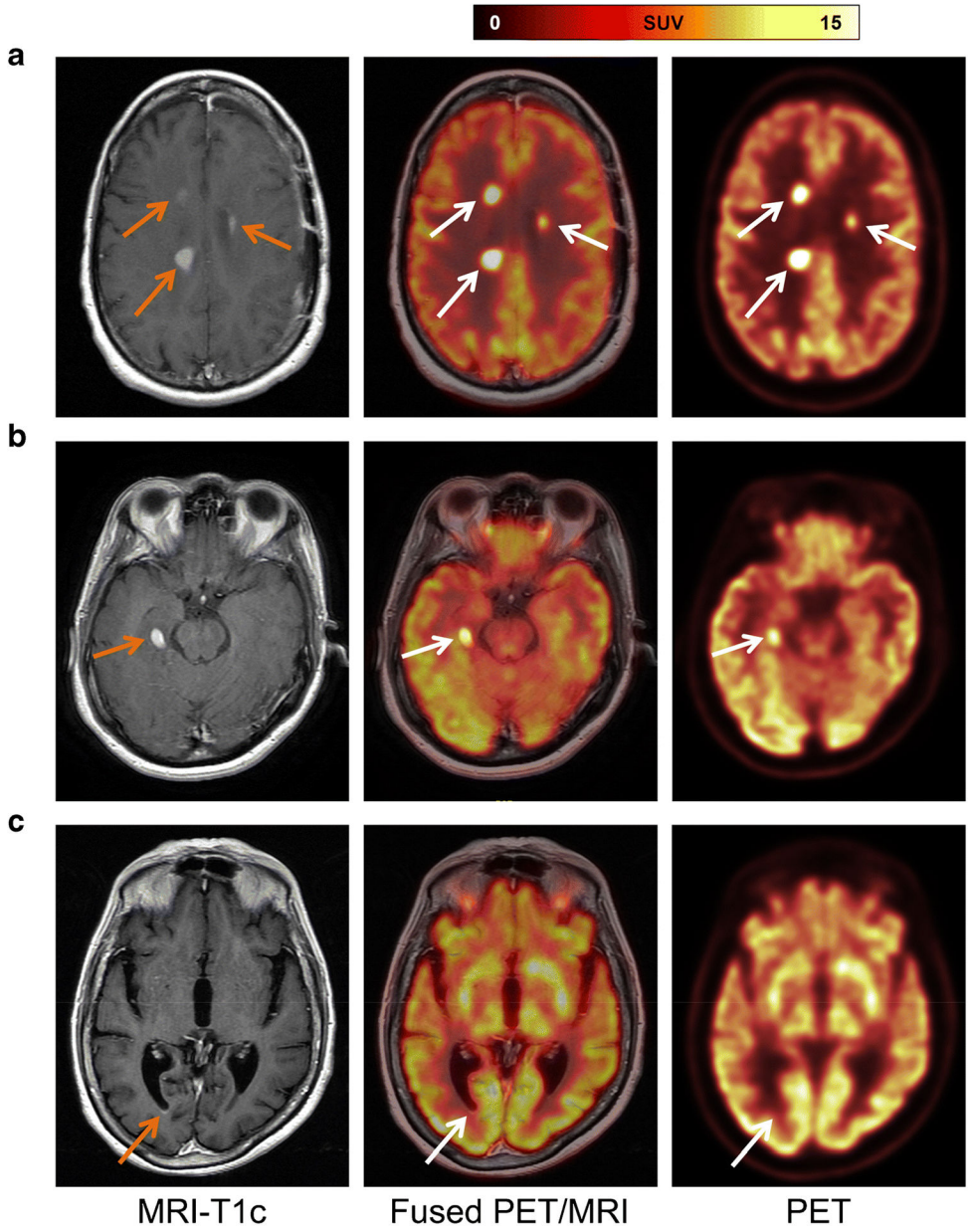

Fig. 2.

Representative cases. (A) Patient diagnosed with secondary CNS lymphoma. Contrast-enhanced T1-weighted MRI shows three enhancing lesions (left, orange arrows), which demonstrate focal [^{18}F]FDG uptake on axial fused PET/MRI (middle, white arrows) and PET images. (B) A representative case of primary CNS lymphoma with a single FDG-avid lesion. Contrast-enhanced T1-weighted MRI depicts an enhancing lesion (left, orange arrow); fused PET/MRI (middle, white arrow) and PET images confirmed focal [^{18}F]FDG uptake. (C) In a patient with primary CNS lymphoma, contrast-enhanced T1-weighted MRI shows a small subependymal enhancement in the right occipital horn (left, orange arrow) that has no correlate on fused PET/MRI (middle, white arrow) or PET images.

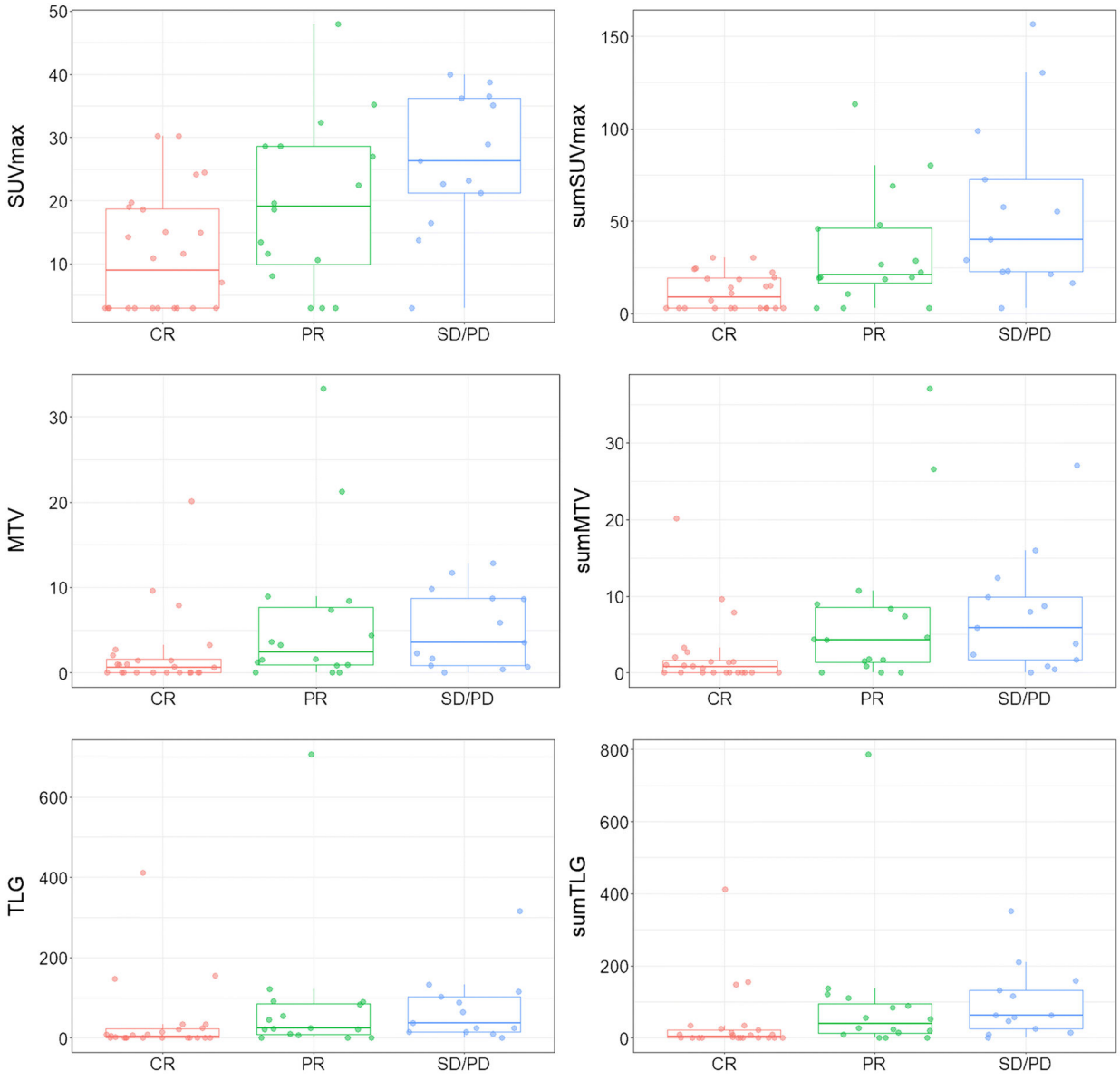

Fig. 3.

Distribution of PET parameters by overall response rate (ORR) for the 53 patients. Center lines show the medians; box limits indicate the 25th and 75th percentiles; whiskers extend 1.5 times the interquartile range from the 25th and 75th percentiles. n = 24, 16, 13.

Table 1.

Patient characteristics

Characteristic	N = 53[1]
CNSL lymphoma	
Primary CNS lymphoma	34 (64%)
Secondary CNS lymphoma	19 (36%)
Sites	
LMD	4 (8%)
parenchymal	26 (49%)
parenchymal+atypical cells	1 (2%)
parenchymal+eye	1 (2%)
parenchymal+LMD	21 (40%)
Age	66 (21, 90)
ECOG	
0	16 (30%)
1	29 (55%)
2	8 (15%)
Gender	
Female	25 (47%)
Male	28 (53%)
Treatment	
Combination	15 (28%)
Single agent	38 (72%)
Number of prior treatments	
0	3 (6%)
1	23 (43%)
2	14 (26%)
3	8 (15%)
4	2 (4%)
5	2 (4%)
8	1 (2%)
MYD88	
Mutated	28 (56%)
Wild type	22 (44%)
Unknown	3
CD79B	
Mutated	21 (41%)
Wild type	30 (59%)
Unknown	2
Total tumor volume (cm3)	1.7 (0.0, 51.3)
Sum of lesions	

Characteristic	N = 53[1]
0	15 (28%)
1	24 (45%)
2	6 (11%)
3	2 (4%)
4	1 (2%)
5	5 (9%)
sumSUVmax	20 (3, 157)
sumMTV	2 (0, 37)
sumTLG	21 (0, 787)
PFS status	
Alive without progression	20 (38%)
Progression/death	33 (62%)
Objective Response	
Complete Response	24 (45%)
Partial Response	16 (30%)
Stable Disease	6 (11%)
Progressive Disease	7 (13%)

[1]Statistics presented: n (%); median (minimum, maximum)

LMD = leptomeningeal disease.

Table 2.

Univariable PFS analysis for PET and clinical parameters, multivariable analysis for PFS in all 53 patients

	Univariable Models				Multivariable Model		
Characteristic	**HR[1]**	**95% CI[1]**	**p-value**	**Characteristic**	**HR[1]**	**95% CI[1]**	**p-value**
SUV_{max}	1.04	1.01, 1.07	0.01				
$sumSUV_{max}$	1.02	1.01, 1.03	<0.001	**$sumSUV_{max}$ (for 5 units)**	1.09	1.04, 1.14	<0.001
log-MTV	1.16	0.96, 1.40	0.13				
log-sumMTV	1.19	0.99, 1.44	0.06				
log-TLG	1.1	0.97, 1.25	0.11				
log-sumTLG	1.12	0.99, 1.26	0.07				
Age	0.99	0.96, 1.01	0.35				
ECOG			0.90				
0	Ref.						
1	1.13	0.51, 2.51					
2	1.29	0.43, 3.89					
Treatment			0.01	**Treatment**			0.02
Combination	Ref.			Combination	Ref.		
Single agent	3.09	1.18, 8.09		Single agent	2.73	1.03, 7.25	
MYD88			0.76				
Mutated	Ref.						
Wild type	0.9	0.44, 1.84					
CD79B			0.73				
Mutated	Ref.						
Wild type	1.14	0.55, 2.35					
N lesions			0.08				
0	Ref.						
1	1.32	0.55, 3.15					
2+	2.78	1.11, 7.00					
log-Total tumor volume (cm^3)	1.16	0.99, 1.35	0.05				

[1]HR = Hazard Ratio, CI = Confidence Interval